

## Experimental study on reinforced sand dune beds Under strip footings

Ahmed M.Gamal<sup>1</sup>, Adel M. Belal<sup>2</sup>, Sameh Abo El-Soud<sup>3</sup>, Ashraf Al-Ashaal<sup>4</sup>  
1,2,3(Construction and Building Engineering Department, College of Engineering and technology/ Arab  
Academy for Science and Technology and Maritime Transport, cairo- Egypt)  
4(National Water Research Center, Director of the Research Institute of Construction, Egypt)

**ABSTRACT:** This paper presents the effect of reinforcement inclusions (geogrids) on the sand dunes bearing capacity under strip footings. In this study the effect of the first geogrid reinforcement depth ( $u/B$ ) and its length ( $L/B$ ) on the bearing capacity will be investigated. Unreinforced bases will also be tested for comparison purposes and determining the bearing capacity ratio (BCR). The results are analyzed to find relationships between the bearing capacity and the geogrid parameters. Laboratory model tests will be carried out on the soil (Sand Dunes) and the inclusion material (geogrid). Experimental work will be carried out on reinforced soil mass to study the interaction between the soil and the geogrid. The results show that the bearing capacity of rigid strip footings on sand dunes can be intensively increased by the inclusion of geogrid layers in the ground, and that the magnitude of bearing capacity increase depends greatly on the geogrid depth ( $u/B$ ) and length ( $L/B$ ). It is also shown that the load-settlement behavior and bearing capacity of the rigid footing can be considerably improved by the inclusion of geogrid at the appropriate location.

**Keywords:** Reinforced soil, Geogrids, Sand Dunes, Bearing Capacity improvement.

### I. INTRODUCTION

The earth reinforcement of, which may be defined as the inclusion of resistant elements in a soil mass to improve its mechanical properties and engineering characteristics. This is especially true on marginal sites with poor foundation soils that would otherwise require prohibitively site improvement measures. Reinforced soil may, for example, be used for construction of new embankments, retention of excavation, stabilization of unstable or sliding slopes, highway construction and improving the soil bearing capacity under footings. Reinforced soil structures results in a coherent and flexible system which make them sustainable to large deformations and seismic loading resistance. [1].

Many researches have been carried out to understand the beneficial effects of using reinforcement in soil, such as, Akinmusuru and Akinbolade (1981)[2], Khing et al. (1993)[3], Omar et al. (1993)[4], Yetimoglu et al. (1994)[5], Boushehrian and Hataf (2003)[6], Bera et al. (2005)[7], Patra et al. (2005)[8], Basudhar et al. (2007)[9], El Sawwaf (2007)[10], Ghazavi and Lavasan (2008)[11], Sharma et al. (2009)[12], G. Madhavi Latha (2009)[13], M.H.A. Mohamed (2010)[14], S.N. Moghaddas Tafreshi (2010)[15], A.F.Zidan (2012)[16] and A.M El-Shesheny (2015)[17]. During the past 30 years, the use of reinforced soils to support shallow foundations has received considerable attention. Many experimental, numerical, and analytical studies have been performed to investigate the behavior of reinforced soil foundation (RSF) for different soil types. However, the behavior of reinforced soil under the foundation has not been established yet. [18]

### II. LABORATORY TECHNIQUES AND MATERIALS

#### 2.1 Sand Dunes

The soil used in this study is Sand dune from Wady Al-Rayan, Alfayoum, Egypt. The sand is classified as SP (poorly graded sand) according to Unified Soil Classification System with coefficient of uniformity ( $C_u$ ) 1.833, coefficient of curvature ( $C_c$ ) 0.89, effective particle size ( $D_{10}$ ) 0.18 mm. The maximum dry unit weight obtained from modified Proctor compaction test was 17.78 kN/m<sup>3</sup> and the minimum dry unit weight obtained by pouring into loosest state was 15.2 kN/m<sup>3</sup>. The friction angle and the cohesion of the sand as determined from direct shear test were found to be 30° and 15 kN/m<sup>2</sup> respectively. Figure 1 and 2 shows the results of the sieve analysis and the direct shear test.

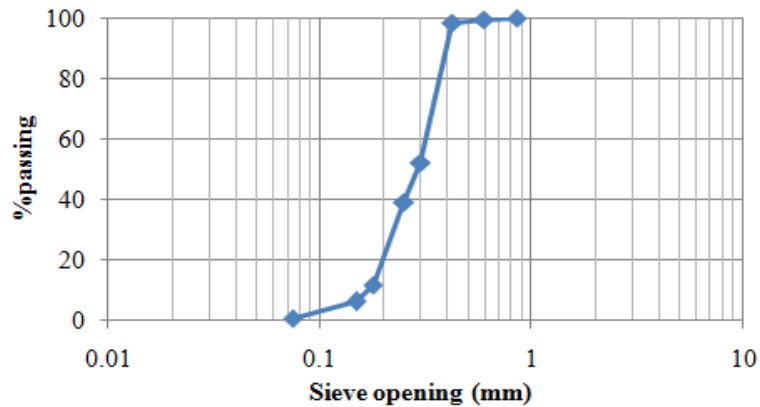


Figure 1: Sieve Analysis results

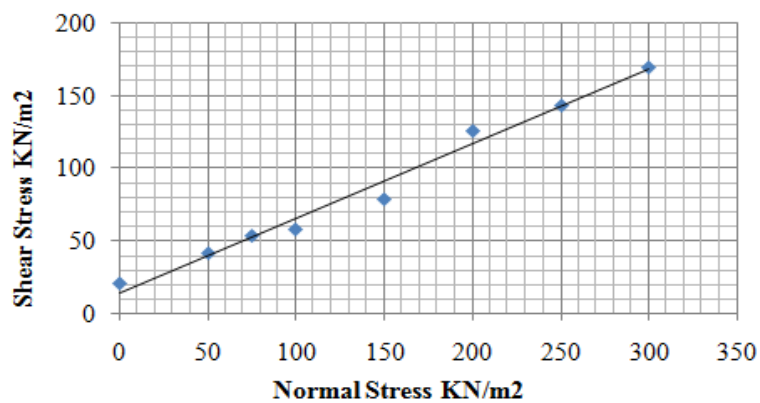


Figure 2: Direct Shear Test Result

**2.2 Geogrids:** In this study the geogrid TENAX TT GS type 045 is used to reinforce the sand dune. It is mono-oriented geogrids manufactured from a unique process of extrusion and especially designed for geosynthetic soil reinforced applications. They are manufactured from high density polyethylene (HDPE) materials and tested to maintain a high tensile modulus, high strength junction, as well as an increased durability against installation damage as shown in figure 3.



Figure 3: TENAX TT 045 GS uniaxial geogrid

Load–elongation behavior of TENAX TT GS was determined from standard multi-rib tension test (ASTM Standard D 6637, 2001) at the National Water Research Center using testometric tension machine. Two methods were used to determine the tensile strength of the geogrid:

**Method A:** Prepare a single rib specimen in the cross-test wide by at least three junctions (two apertures) long in the direction of the testing as shown if figure 4. [19]

**Method B:** Prepare a five rib specimen with a minimum of 200 mm wide and contain 5 ribs in the cross-test direction wide by at least 3 junctions (two apertures) or 300 mm (12in) long in the direction of the testing, as shown in figure 5. [19]



**Figure 4:** Specimen prepare for Method A



**Figure 5:** Specimen prepare for Method B

Junction and rib failure are the two modes of failure for the geogrid when they are subjected to tensile as shown in Figure 6 and Figure 7 respectively.



**Figure 6:** Geogrid Junction Rupture

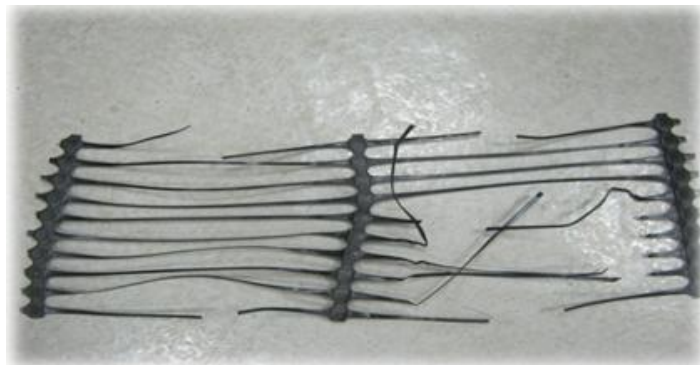


**Figure 7:** Geogrid Rib Rupture

### 2.2.1 Geogrid test result

The testometric materials testing machine software extracts a result report showing the force at peak (N), the corresponding strain (%), the ASTM D 6637 tensile strength and the secant stiffness (%). Figure 8 and Figure 9 shows the test report for TENAX TT 045 GS uniaxial geogrid results for method (A) and method (B) respectively.

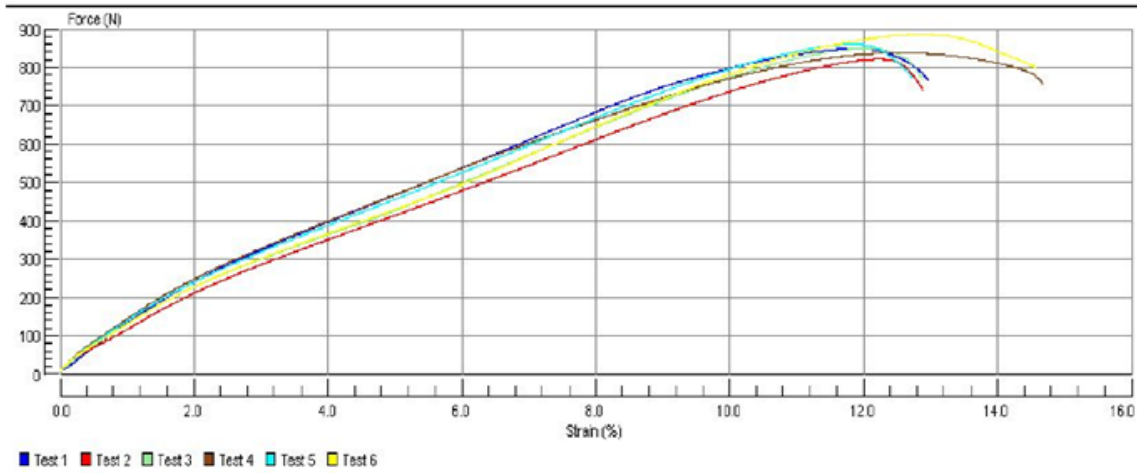


Figure 8: Results of TENAX TT 045 GS uniaxial (Method A)

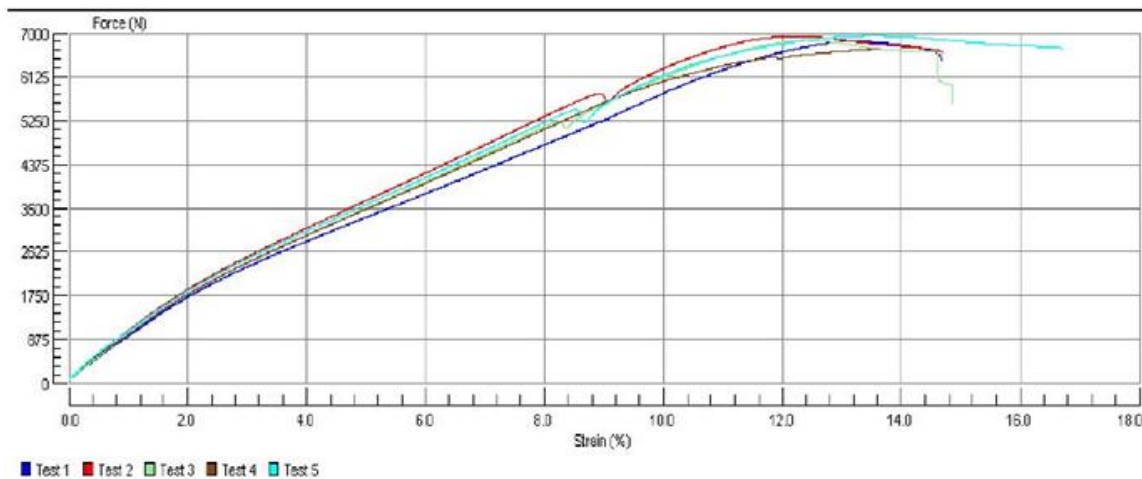


Figure 9: Results of TENAX TT 045 GS uniaxial (Method B)

For the single rib test result (Method A), the mean force at peak 851 N with a strain 13.45 % and for the multi-rib test result (Method B) the mean force at peak 6851.6 N with strain 14.913 % and ASTM D 6637 Tensile Strength 40595.730 N/m. the results shows an agreement with the data sheet provided by the supplier.

## III. EXPERIMENTAL STUDY ON REINFORCED BED

Various laboratory tests were made on the reinforced soil bed in order to study the soil/geogrid interaction and to analysis the results for the case of reinforced and unreinforced soil bed.

### 3.1 Laboratory model test setup

#### 3.1.1 Box Model

The main elements of the laboratory apparatus are a tank, a steel frame with a horizontal steel beam over the tank. The test box, having inside dimensions of 1200 mm X 400 mm X1200 mm and 5mm thickness is made from steel with the front wall made of 10 mm thickness plexi-glass and is supported directly on two steel angles as shown in Figure 10. These dimensions was designed to ensure the rigidity of the steel tank The glass side allows the sample to be seen during preparation and sand particle deformations to be observed during testing. The tank box was built sufficiently rigid to maintain plane strain conditions by minimizing the out of plane displacement.

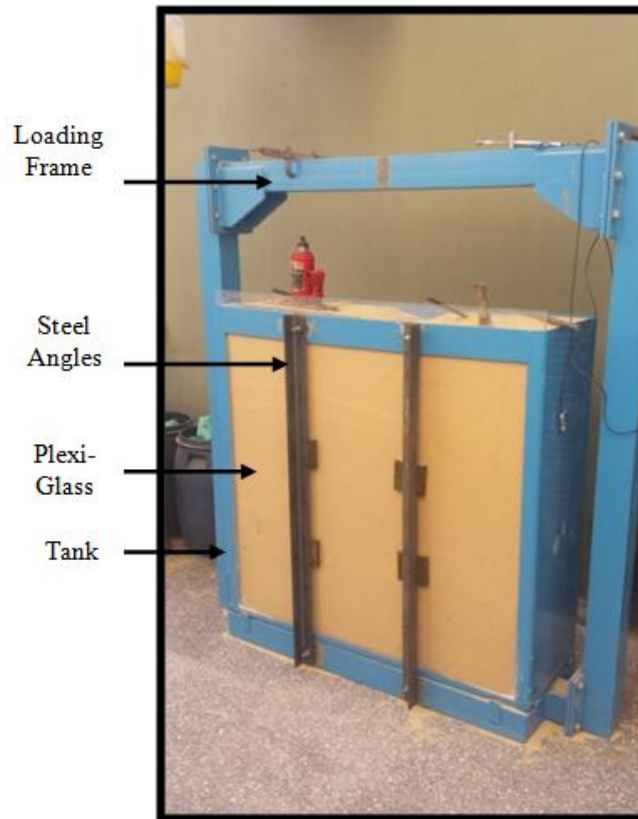


**Figure 10:** Model Box

### 3.1.2 Footing Model

Three rigid 10 mm thick of steel plate model strip footing (A): 75mmX380mm, (B): 100mmX380mm (C): 120mmX380mm. They are used in the experimental model to study the effect of the footing dimensions on the mechanical behavior of the reinforced soil mass as shown in Figure 11.



**Figure 11:** Model footings

### 3.1.3 Loading system

A 10 ton manual hydraulic jack with a stroke length of 220 mm is placed on the footing against a reaction frame to push the footing slightly into the bed for proper contact between the soil and the footing as shown in Figure 12.

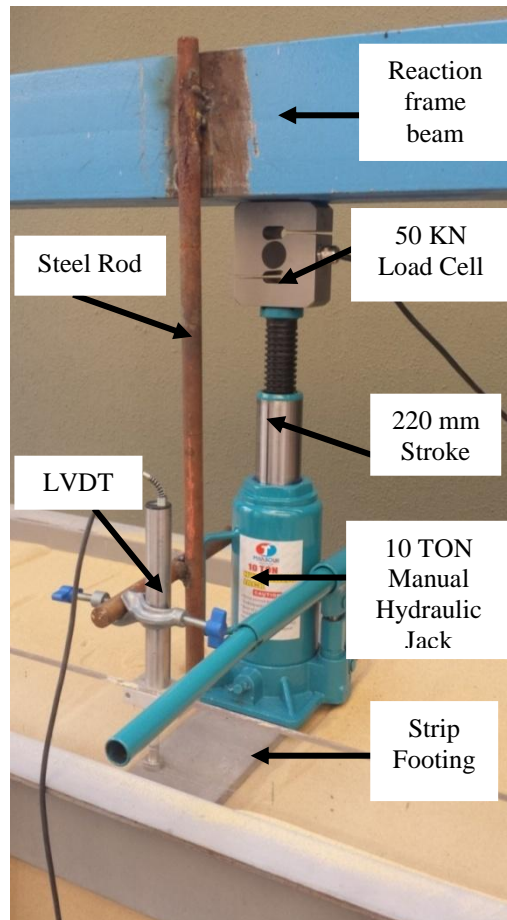


Figure 12: The loading system with measuring instruments

### 3.1.4 Measuring instruments

A 50 kN load cell is placed between the stroke of the manual hydraulic jack and the beam of the reaction frame for measuring the load in kN. A displacement transducer (LVDT) is placed on the footing and attached to a vertical steel rod to ensure the verticality of the LVDT to avoid miss readings in the displacement. The load cell and the LVDT are connected to an electronic 8 channel data acquisition unit as shown in Figure 13. The readings were displayed and saved by the data logger software. The load cell and the LVDT are calibrated according to a calibration sheet.



Figure 13: Data acquisition unit

### 3.1.5 Preparation of test bed

The sand was placed in the test tank by free fall into 6 layers. Each layer is 200 mm thick. Each layer is compacted using the modified proctor hammer which is dropped on a rigid 10 mm thick steel plate with dimensions of 300 mm X 380 mm and area of 114000 mm<sup>2</sup> rested on the soil surface. Each layer was compacted 30 blows/ 144000 mm<sup>2</sup>. Choosing the number of layers, the layer thickness and the number of blows is based on several trials in order to maintain the maximum dry unit weight 17.78 kN/m<sup>2</sup>. Figure 14 shows the preparation of the test bed.

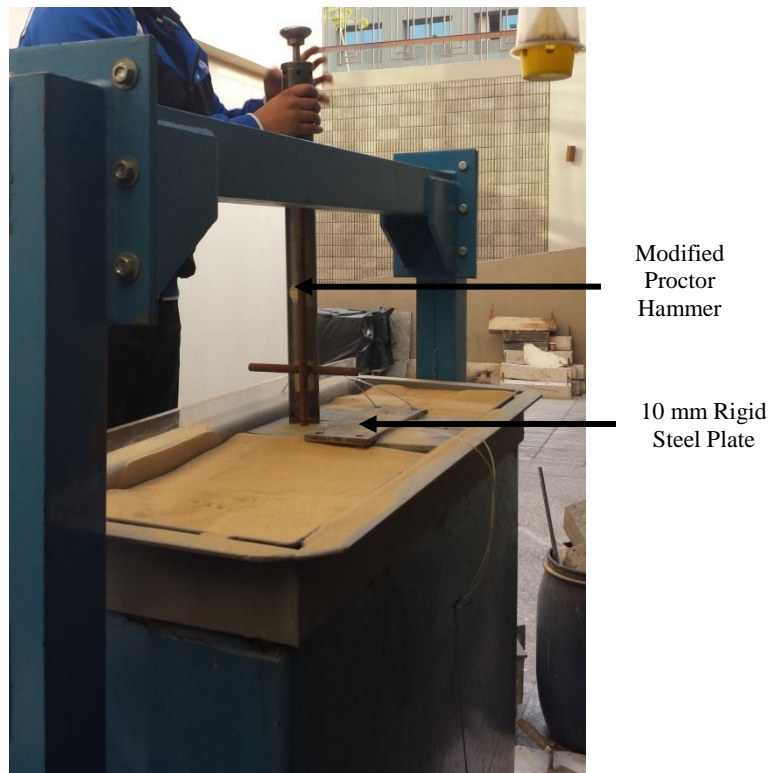


Figure 14: Preparation of sand bed

### 3.1.6 Geogrid layout and preparation

In this study the distance of the 1<sup>st</sup> geogrid layer to the footing ( $u$ ) and the length of the geogrid ( $L$ ) is variable to study their effect on the soil/geogrid mechanical behavior as shown in Figure 15. For each test about 5 times the footing width ( $B$ ) of the soil bed is removed from the tank. The sand is then placed and compacted into layers till the level of the geogrid is reached which is  $(u/B)=0.25, 0.5$  and  $0.75$ . Figure 16a, Figure 16b shows the geogrid layout.

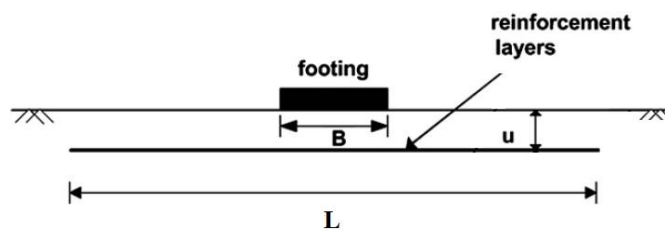


Figure 15: Geogrid layout



Figure 16a: Geogrid preparation ( $L/B=12$ )



Figure 16b: Geogrid preparation ( $L/B=2.5$ )

3.2 Experimental model matrix

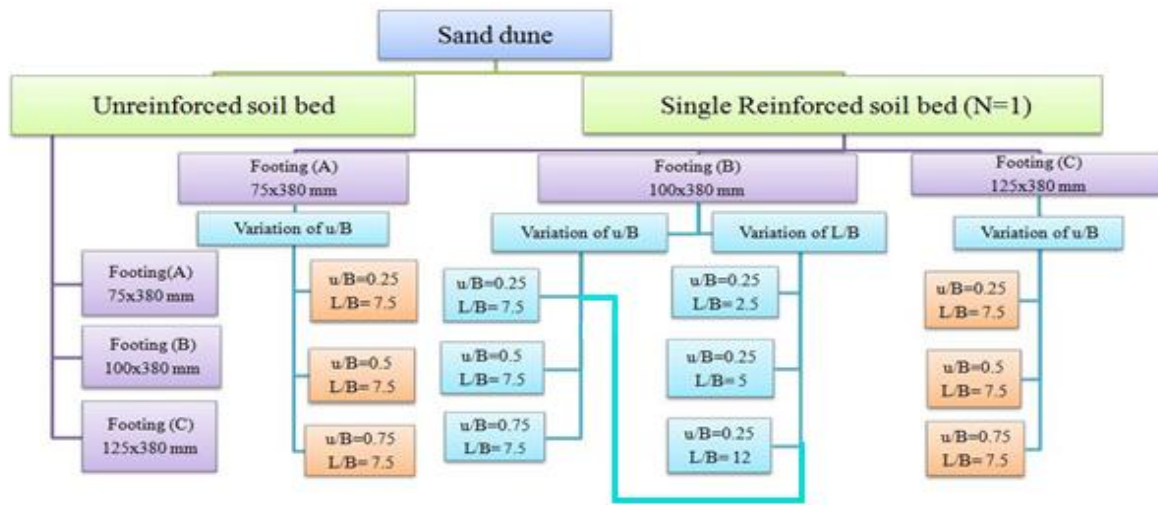


Figure 17: Experimental model matrix

3.3 Experimental model results

3.3.1 Unreinforced soil bed

Figure 18 and table 1 shows the results from the experimental model for the unreinforced soil bed with the footing A, B and C. It is noticed that as the width of the footing increases the stress at failure increases which agrees with Terzaghi ultimate bearing capacity criteria.

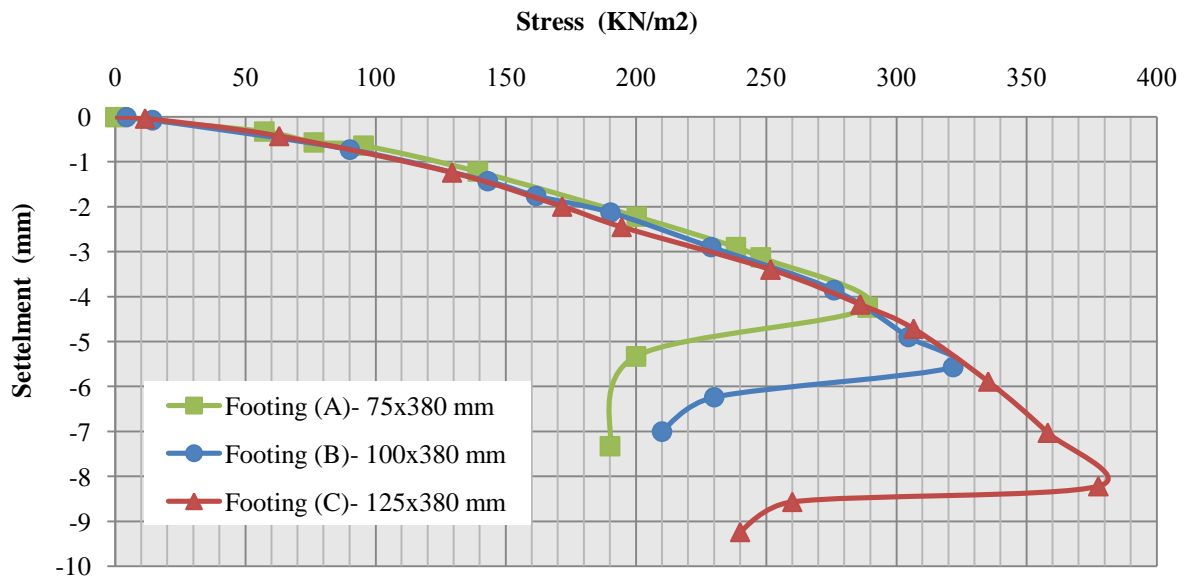


Figure 18: Unreinforced Soil bed Experimental results

Table 1: Unreinforced Soil bed Experimental results

Footing	Failure stress (KN/m2)	Settlement (mm)
A	288	4.2
B	322	5.6
C	378	8.2

3.3.2 Reinforced soil bed

3.3.2.1 Effect of u/B with Footing (A)

Figure 19 and table 2 shows footing (A) experimental model results of u/B=0.25, 0.5, and 0.75 for L/B=7.5.

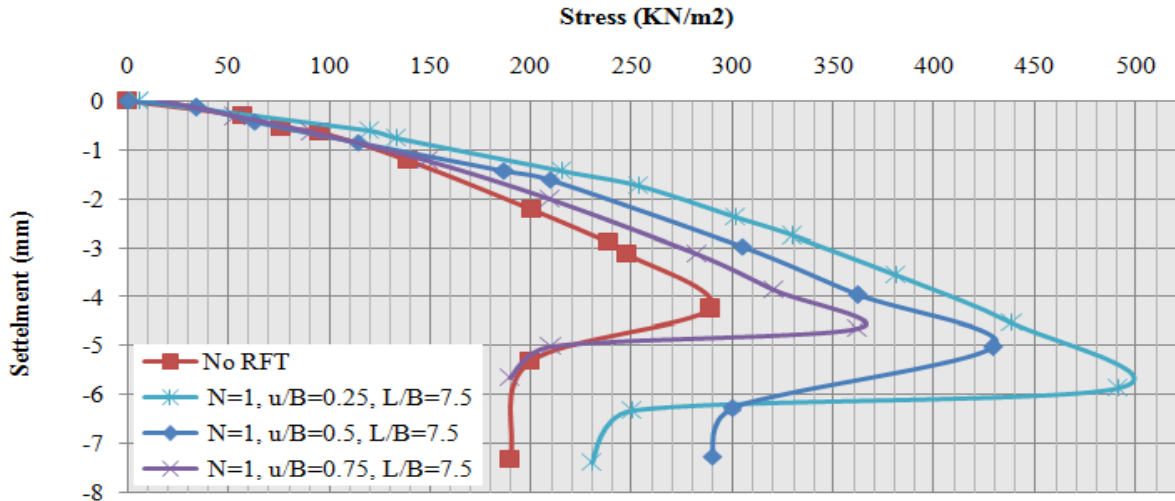


Figure 19: Variation of u/B with footing (A) Experimental Results

Table 2: Variation of u/B with footing (A) Experimental Results

	No. of Geogrids (N)	Variable Parameter (u/B)	Constant Parameter (L/B)	Failure stress (KN/m <sup>2</sup> )	Settlement (mm)
Footing A	1	0.25	7.5	491	5.9
		0.5		429	5
		0.75		362	4.6

3.3.2.2 Effect of u/B with footing (B)

Figure 20 and table 3 shows footing (B) experimental model results of u/B=0.25, 0.5, and 0.75 for L/B=7.5.

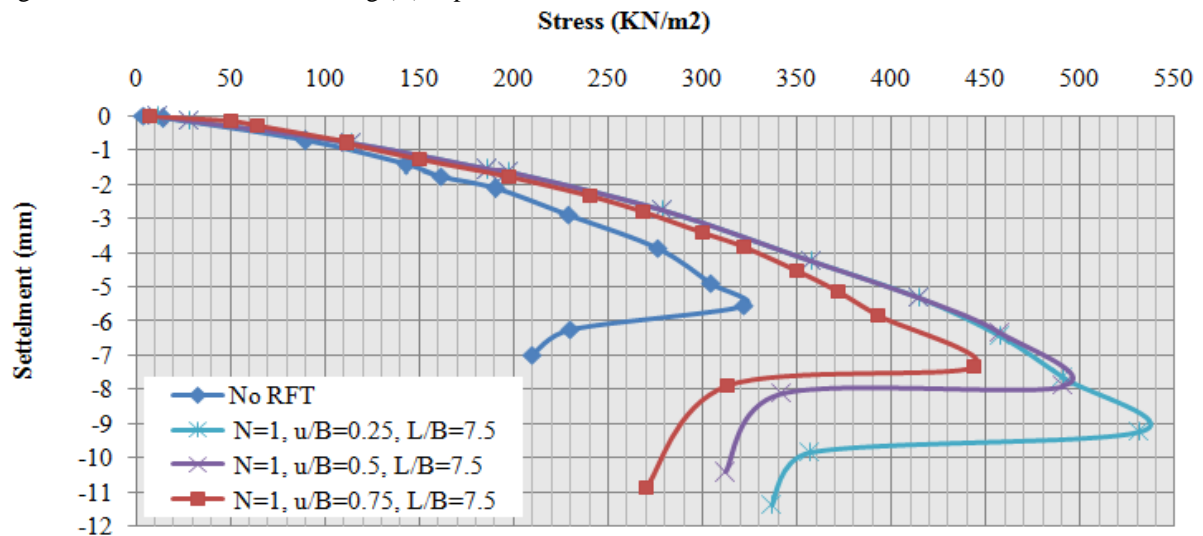


Figure 20: Variation of u/B with footing (B) Experimental Results

Table 3: Variation of u/B with footing (B) Experimental Results

	No. of Geogrids (N)	Variable Parameter (u/B)	Constant Parameter (L/B)	Failure stress (KN/m <sup>2</sup> )	Settlement (mm)
Footing B	1	0.25	7.5	540	9.6
		0.5		490	7.8
		0.75		443	7.3

3.3.2.3 Effect of u/B with footing (C)

Figure 21 and table 4 shows footing (C) experimental model results of u/B=0.25, 0.5, and 0.75 for L/B=7.5.

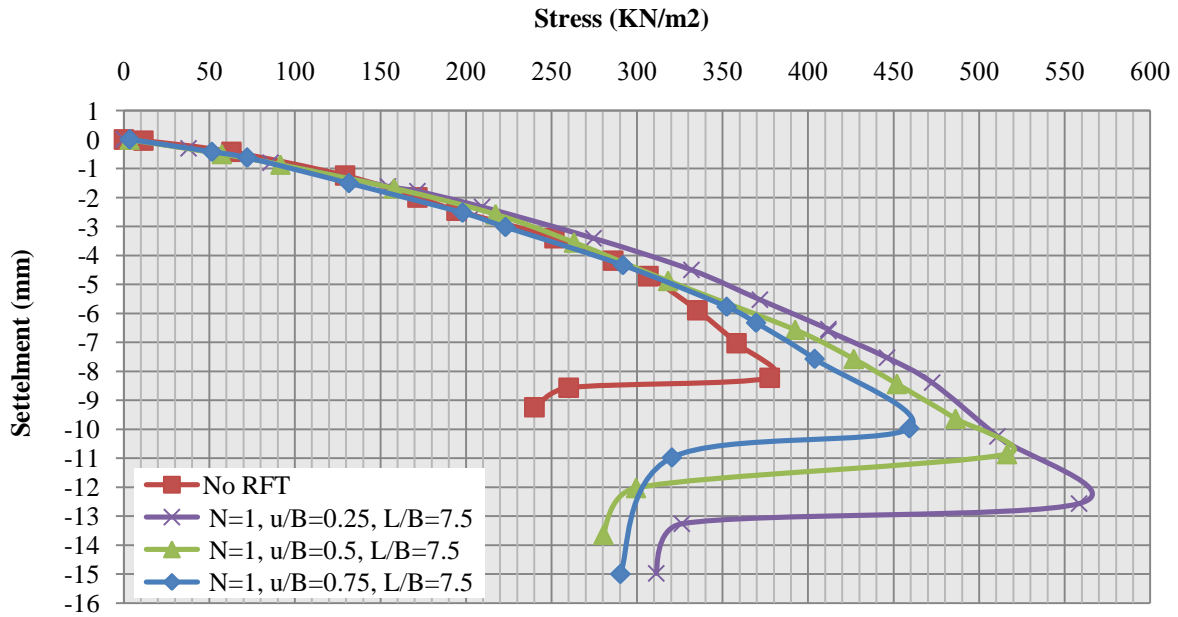


Figure 21: Variation of u/B with footing (C) Experimental Results

Table 4: Variation of u/B with footing (C) Experimental Results

Footing C	No. of Geogrids (N)	Variable Parameter (u/B)	Constant Parameter (L/B)	Failure stress (KN/m <sup>2</sup> )	Settlement (mm)
	1	0.25	7.5	558	12.5
0.5	516	10.8			
0.75	459	9.9			

It is noticed that for footing (A), (B) and (C) as the geogrid reinforcement is closer to the footing level the stress at failure increase, therefore improvement of the sand dune bearing capacity

3.3.2.4 Effect of L/B with footing (B)

Figure 22 and table 5 shows footing (B) experimental model results of L/B= 2.5, 5, 7.5, and 12 for u/B=0.25

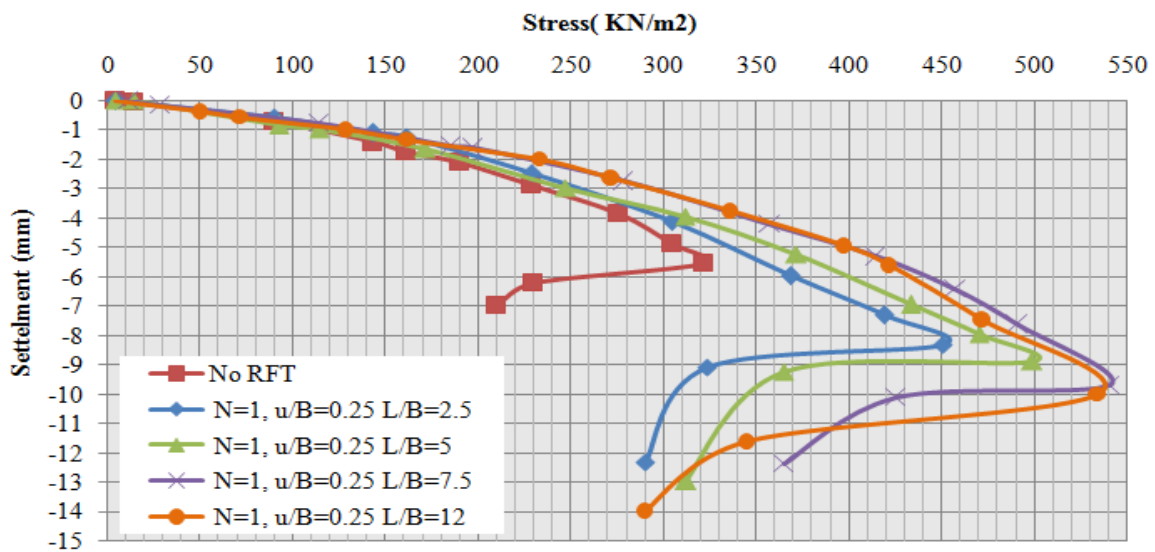


Figure 22: Variation of L/B with footing (B) Experimental Results

**Table 5:** Variation of L/B with footing (B) Experimental Results

Footing B	No. of Geogrids (N)	Variable Parameter (L/B)	Constant Parameter (u/B)	Failure stress (KN/m <sup>2</sup> )	Settlement (mm)
	1		2.5	0.25	450
5			499		8.9
7.5			540		9.7
12			522		10

It can be noticed that as the width of the geogrid reinforcement increases the stress at failure increases until the geogrid length (L) reaches 7.5B. It is also noticed that L/B=7.5 and 12 are having almost the same trend which means using geogrid length 7.5B is sufficient

#### IV. RESULT ANALYSIS AND DISCUSSION

##### 4.1 Effect of first reinforcing layer depth:

In this study, the depth of the first reinforcing layer has been changed for L/B=7.5 to get the optimum depth. Table 6 shows the Variation in the depth of the first reinforcing layer for L/B=7.5 with footing (A), (B) & (C)

**Table 6:** Variation in the depth of the first reinforcing layer

Footing Width (B)	N	1			
		u/B	0.25	0.5	0.75
		L/B	7.5	7.5	7.5
75 mm		u (mm)	18.75	37.5	56.25
		L (mm)	562.5	562.5	562.5
100 mm		u (mm)	25	50	75
		L (mm)	750	750	750
125 mm		u (mm)	31.25	62.5	93.75
		L (mm)	937.5	937.5	937.5

It can be concluded that the effect of using u/B = 0.25 is the optimum for footing (A), (B) & (C)

##### 4.2 Effect of reinforcing layers width:

In this study, the width of the first reinforcing layer has been changed for u/B=0.25 to get the optimum width. Table 7 shows the Variation in the width of the first reinforcing layer for u/B=0.25 with Footing (A), (B) & (C)

**Table 7:** Variation in the width of the first reinforcing layer

Footing Width (B)	N	1				
		L/B	2.5	5	7.5	12
		u/B	0.25	0.25	0.25	0.25
75 mm		L (mm)	187.5	375	562.5	900
		u (mm)	18.75	18.75	18.75	18.75
100mm		L (mm)	250	500	750	1200
		u(mm)	25	25	25	25
125mm		L (mm)	312.5	625	937.5	1500
		u (mm)	31.25	31.25	31.25	31.25

It can be concluded that the effect of using L/B = 7.5 and 12 is almost the same therefore effect of using L/B=7.5 is the optimum for footing (A), (B) & (C)

### 4.3 Bearing capacity ratio (BCR)

The BCR of the footing on the reinforced sand is represented using a non-dimensional factor, called bearing capacity ratio BCR. This factor is defined as the ratio of the footing ultimate pressure with reinforced bed ( $q_u$  reinforced) to the footing ultimate pressure with the unreinforced bed ( $q_u$  unreinforced).

Figure 23 illustrates the BCR of the soil versus variable values of  $u/B$  for footings (A), (B) and (C). It is noticed that the values of (BCR) for  $u/B=0.25$ , and  $L/B=7.5$  are 1.7, 1.6 and 1.5 respectively, therefore 50-70% improvement. That means as the width of the footing decrease the improvement of the BCR increase.

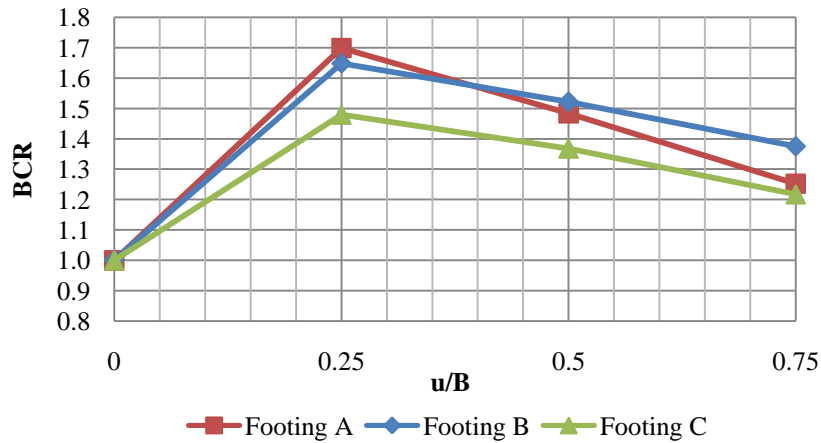


Figure 23: BCR vs.  $u/B$  for footing (A), (B) & (C)

Figure 24 illustrates the BCR of the soil versus variable values of  $L/B$  for footing (B). It is noticed that the values of (BCR) for  $L/B=7.5$  and  $u/B=0.25$  improves the sand dunes bearing capacity by 60% for footing (B). That means as the width of the reinforcement increase, the improvement of the BCR increase up to  $L/B = 7.5$ .

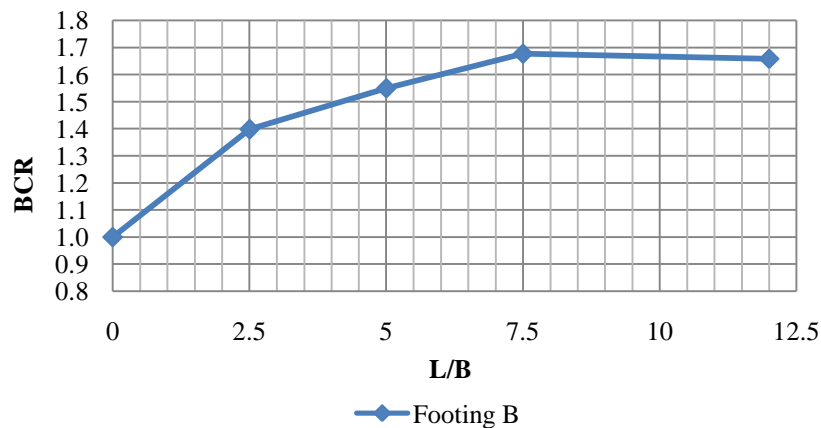


Figure 24: BCR vs.  $L/B$  for footing (B)

## V. CONCLUSIONS

A Series of model tests has been carried out to evaluate the bearing capacity of a strip footing resting on georeinforced sand dunes. The study aimed at determining the effect of geogrid reinforcements and its location on the bearing capacity and settlement characteristics of such footings. Based on the results from this investigation, the following conclusions can be drawn:

- Experimental study on single reinforced sand dune beds under strip footings shows a sufficient improvement in the bearing capacity
- The results analysis shows the Bearing capacity ratio (BCR) 1.7, 1.6 and 1.5 for footing A, B and C respectively that is 50-70 % improvement
- The result analysis shows a higher BCR for footing (A) compared to footing (B) and footing (C), therefore the reinforced soil technique appeared to be efficient for smaller strip footings

- The optimum embedment depth of geogrid sheet from the footing resulted in the maximum ultimate bearing capacity of the reinforced soil mass is about 0.25 times the width of the footing.
- The optimum length geogrid sheet resulted in the maximum ultimate bearing capacity of the reinforced soil mass is about 7.5 times the width of the footing.

#### REFERENCES

- [1]. James K. Mitchell “Reinforcement of earth slopes and embankments”, June 1987.
- [2]. Akinmusuru, J.O., Akinbolade, J.A., Stability of loaded footings on reinforced soil. *Journal of the Geotechnical Engineering Division, ASCE* 107 (6), 1981, 819–827
- [3]. Khing, K.H., Das, B.M., Puri, V.K., Cook, E.E., Yen, S.C., The bearing capacity of a strip foundation on geogrid reinforced sand. *Geotextiles and Geomembranes* 12, 1993, 351–361.
- [4]. Omar, M.T., Das, B.M., Puri, V.K., Yen, S.C., Ultimate bearing capacity of shallow foundations on sand with geogrid reinforcement. *Canadian Geotechnical Journal* 30, 1993, 545–549.
- [5]. Yetimoglu, T., Wu, J.T.H., Saglamer, A., Bearing capacity of rectangular footings on geogrid-reinforced sand. *Journal of Geotechnical Engineering, ASCE* 120, 1994, 2083–2099.
- [6]. Boushehrian, J.H., Hataf, N., Experimental and numerical investigation of the bearing capacity of model circular and ring footings on reinforced sand. *Geotextiles and Geomembranes* 23 (2), 2003, 144–173.
- [7]. Bera, A.K., Ghosh, A., Ghosh, A., Regression model for bearing capacity of a square footing on reinforced pond ash. *Geotextiles and Geomembranes* 23 (3), 2005, 261–285.
- [8]. Patra, C.R., Das, B.M., Atalar, C., Bearing capacity of embedded strip foundation on geogrid-reinforced sand. *Geotextiles and Geomembranes* 23, 2005, 454–462.
- [9]. Basudhar, P.K., Saha, S., Deb, K., Circular footings resting on geotextile-reinforced sand bed. *Geotextiles and Geomembranes* 25 (6), 2007, 377–384.
- [10]. El Sawwaf, M.A., Behavior of strip footing on geogrid-reinforced sand over a soft clay slope. *Geotextiles and Geomembranes* 25 (1), 2007, 50–60.
- [11]. Ghazavi, M., Lavasan, A.A., Interference effect of shallow foundations constructed on sand reinforced with geosynthetics. *Geotextiles and Geomembranes* 26 (5), 2008, 404–415.
- [12]. Sharma, R., Chen, Q., Abu-Farsakh, M., Yoon, S., Analytical modeling of geogrid reinforced soil foundation. *Geotextiles and Geomembranes* 27, 2009, 63–72
- [13]. G. Madhavi Latha, Amit Somwanshi, Effect of reinforcement form on the bearing capacity of square footings on sand, *Geotextiles and Geomembranes* 27(2009) 409–422.
- [14]. M.H.A. Mohamed, Two dimensional experimental study for the behaviour of surface footings on unreinforced and reinforced sand beds overlying soft pockets, *Geotextiles and Geomembranes* 28, 2010, 589-596.
- [15]. S. Tafreshi and A. Dawson, Behaviour of footings on reinforced sand subjected to repeated loading—Comparing use of 3D and planar geotextile, *Geotextiles and Geomembranes*, vol. 28, pp. 434-447, 2010.
- [16]. A. Zidan, Numerical study of behavior of circular footing on geogrid-reinforced sand under static and dynamic Loading, *Geotechnical and Geological Engineering*, vol. 30, pp. 499-510, 2012.
- [17]. A.M El-Shesheny “Finite Element Analysis of Reinforced Soil under Dynamic loads”, Feb 2015
- [18]. Radhey Sharma, Qiming Chen, Murad Abu-Farsak, Sungmin Yoon, Analytical modeling of geogrid reinforced soil foundation”, *Geotextiles and Geomembranes* 27 (2009) 63–72
- [19]. ASTM Standard D 6637, 2001. Standard Test Method for Determining Tensile Properties of Geogrids by the Single Or Multi-rib Tensile Method. American Society for Testing and Materials, Pennsylvania, USA.